Nucleic Acids Research, 2005, Vol. 33, No. 21 ***6837–6849***
doi:10.1093/nar/gki991

Cell-penetrating peptide conjugates of peptide nucleic acids (PNA) as inhibitors of HIV-1 Tat-dependent *trans*-activation in cells

John J. Turner, Gabriela D. Ivanova, Birgit Verbeure, Donna Williams, Andrey A. Arzumanov, Saïd Abes[1], Bernard Lebleu[1] and Michael J. Gait*

Laboratory of Molecular Biology, Medical Research Council, Hills Road, Cambridge CB2 2QH, UK and [1]UMR 5124 CNRS, CC 086, Université Montpellier 2, Place Eugène Bataillon, 34095 Montpellier, France

Received October 6, 2005; Revised and Accepted November 14, 2005

ABSTRACT

The *trans*-activation response (TAR) RNA stem–loop that occurs at the 5′ end of HIV RNA transcripts is an important antiviral target and is the site of interaction of the HIV-1 Tat protein together with host cellular factors. Oligonucleotides and their analogues targeted to TAR are potential antiviral candidates. We have investigated a range of cell penetrating peptide (CPP) conjugates of a 16mer peptide nucleic acid (PNA) analogue targeted to the apical stem–loop of TAR and show that disulfide-linked PNA conjugates of two types of CPP (Transportan or a novel chimeric peptide R_6-Penetratin) exhibit dose-dependent inhibition of Tat-dependent *trans*-activation in a HeLa cell assay when incubated for 24 h. Activity is reached within 6 h if the lysosomotropic reagent chloroquine is co-administered. Fluorescein-labelled stably-linked conjugates of Tat, Transportan or Transportan TP10 with PNA were inactive when delivered alone, but attained *trans*-activation inhibition in the presence of chloroquine. Confocal microscopy showed that such fluorescently labelled CPP–PNA conjugates were sequestered in endosomal or membrane-bound compartments of HeLa cells, which varied in appearance depending on the CPP type. Co-administration of chloroquine was seen in some cases to release fluorescence from such compartments into the nucleus, but with different patterns depending on the CPP. The results show that CPP–PNA conjugates of different types can inhibit Tat-dependent *trans*-activation in HeLa cells and have potential for development as antiviral agents. Endosomal or membrane release is a major factor limiting nuclear delivery and *trans*-activation inhibition.

INTRODUCTION

Efficient delivery of oligonucleotides and their analogues through cell membranes to allow interaction with intracellular RNA targets and to control gene expression has proved to be a significant challenge. Oligonucleotide analogues that carry negative charges (e.g. phosphodiesters or phosphorothioates) are often delivered into common laboratory cell lines in culture (such as HeLa cells) by complexation with cationic lipids (1), of which there is now a wide choice. However, there are usually limiting lipid-associated cell toxicities and stability disadvantages for therapeutic use. Charge-neutral peptide nucleic acids (PNAs) (2) and phosphorodiamidate morpholino oligomers (PMO) (3) have been developed as oligonucleotide analogues that are unaffected by cellular nucleases and which have strong RNA binding. It was hoped that the lack of negative charge might facilitate cell uptake, but cell membrane translocation of unmodified PNA and PMO has proved to be as inefficient as for phosphate-containing oligonucleotides and analogues (4).

Recently, certain peptides [known as cell penetrating peptides (CPPs) or protein transduction domains] have been identified that have strong cell translocation properties and potential for drug delivery (5). A number of promising cell delivery studies have focussed on covalent conjugates of CPPs with various types of cargo [reviewed in Refs (6–8)] including oligonucleotides and their analogues [reviewed in Refs (9–11)]. Whereas conjugates of CPPs with negatively charged

*To whom correspondence should be addressed. Tel: +44 1223 248011; Fax: +44 1223 402070; Email: mgait@mrc-lmb.cam.ac.uk
Present address:
Birgit Verbeure, Centre for Intellectual Property Rights, Catholic University of Leuven, Minderbroederstraat 5, B-3000 Leuven, Belgium

phosphodiester or phosphorothioate oligonucleotides have had mixed results in recent cell delivery studies (12–15), several reports have showed enhanced cellular delivery and biological activity of PNA covalently attached to CPPs [reviewed in Refs (9,11)].

In common with many other steric block oligonucleotide analogue types, PNA does not induce RNase H-dependent RNA cleavage when bound to an RNA target. Therefore stoichiometric amounts must be delivered into either the cytosol of cells [e.g. to block translation (16)] or into the nucleus [e.g. to redirect splicing (17)] compared with the amount of target RNA. Thus, efficient delivery is of paramount importance to observe strong gene expression control effects.

For some years we have studied the *trans*-activation activity of the HIV-1 *trans*-activator protein Tat which interacts with the HIV *trans*-activation responsive element (TAR) stem–loop RNA and other cellular factors to strongly stimulate transcriptional elongation from the viral long terminal repeat (LTR) (18,19). Inhibitors of these RNA–protein interactions block full-length transcription and resultant HIV-1 gene expression, and thus are potential candidates for anti-HIV therapies. Despite much effort to date, no small molecule inhibitors [reviewed in Refs (20)] have emerged as clinical candidates.

Several years ago, we showed that 12mer steric block oligonucleotide analogues of a number of types [e.g. 2′-*O*-methyl (OMe), a mixmer oligonucleotide containing OMe and some 5-methyl C locked nucleic acid (LNA) units, or a PNA oligomer] targeted to the apical part of the TAR stem–loop, which is highly sequence-conserved (Figure 1), were able to inhibit sequence-specifically Tat-dependent *in vitro* transcription directed by HeLa cell nuclear extract on a DNA template containing the HIV-1 LTR (21–23). We then showed that, when delivered by a cationic lipid or surfactant, 12mer and 16mer OMe/LNA mixmer oligonucleotides could dose-dependently and sequence-dependently inhibit Tat-dependent HIV LTR *trans*-activation from a stably integrated plasmid system in HeLa cells with a firefly luciferase reporter, but without effect on a control *Renilla* luciferase reporter (22,23). Fluorescein-labelled OMe/LNA oligonucleotides were found by confocal microscopy to be located in both cytosolic and nuclear compartments when delivered by a range of cationic lipid reagents (23).

Recently, we described the chemical synthesis and purification of disulfide conjugates of a range of CPPs with fluorescein-labelled OMe/LNA oligonucleotides and reported that in all cases such conjugates were unable to inhibit Tat-dependent *trans*-activation in our HeLa cell reporter assay involving stably integrated reporter plasmids (15). Whereas in most cases attachment of a CPP significantly enhanced unassisted HeLa cell uptake of the oligonucleotides, their uptake was confined to cytosolic (presumably endosomal) compartments. Exclusion from the cell nucleus correlated with the lack of inhibition of Tat-dependent *trans*-activation, suggesting that the barrier to nuclear activity is due to insufficient release from endosomal compartments. Similar cytosolic entrapment was also a feature of OMe/LNA oligonucleotide lipid-free uptake studies into human fibroblasts (15).

Kaushik *et al*. (24) found that 15mer and 16mer steric block PNAs targeted to the TAR RNA, when electroporated into CEM lymphocytes, were able to inhibit Tat-dependent *trans*-activation in a transient luciferase reporter assay and also block expression of luciferase from CEM cells pre-infected with pseudotyped HIV-1 virions. 16mer PNA disulfide conjugated to the CPP Transportan [a synthetic chimeric peptide derived from the neuropeptide galanin and wasp venom toxin mastoparan (25)] inhibited Tat-dependent *trans*-activation in Jurkat or CEM cells or Jurkat cells transiently transfected with luciferase reporters (IC_{50} of ~0.5 μM), and also inhibited HIV-1 production in chronically infected H9 cells (IC_{50} of ~1 μM), where it appeared to be acting by inhibition at the transcriptional level (26). Subsequently, Chaubey *et al*. (27) have shown improved activity levels of the same PNA-Transportan conjugate in an antiviral assay in blocking synthesis of proviral DNA and significantly higher level of activity (IC_{50} of ~40 nM) by inhibition of viral infectivity by pre-treatment of HIV virions.

Our current studies address the important question of how the chemical structure of a CPP–PNA (the type of CPP, its placement and the type of linkage) relates to its ability to penetrate HeLa cells, enter the nucleus and inhibit Tat-dependent *trans*-activation, which is one of the proposed mechanisms for attaining antiviral activity. We now report the chemical synthesis of a range of CPPs conjugated either through a stable polyether or through a cleavable disulfide linkage to a 16mer PNA targeted to the HIV-1 TAR apical loop. We study their ability to inhibit Tat-dependent *trans*-activation when incubated with HeLa cells using a rigorous, double-luciferase reporter system that involves stably integrated plasmids. We show that disulfide-linked CPP–PNA conjugates with two types of CPP (Transportan or a novel chimeric peptide R_6-Penetratin) are able to inhibit Tat-dependent *trans*-activation when incubated with HeLa cells for 24 h. Co-administration of the lysosomotropic reagent chloroquine allowed activity to be seen within 6 h. In addition, *trans*-activation inhibition could be attained for several FAM-labelled, stably-linked CPP–PNA conjugates, notably Tat-PNA, in the presence of chloroquine, which were inactive in its absence. Confocal microscopy showed that such CPP–PNA conjugates, when incubated with Hela cells in the absence of chloroquine, were sequestered in endosomal or membrane-bound compartments of HeLa cells, which varied in appearance depending on the CPP type. In some cases, co-administration of chloroquine was seen to release fluorescence from such compartments into the nucleus, but with different patterns depending on the CPP. The results are significant in that CPP–PNA conjugates of different types can inhibit Tat-dependent *trans*-activation in cells and that endosome or membrane release is a major factor limiting nuclear delivery and *trans*-activation inhibition. The results contribute towards improved design of biologically active CPP–PNA.

MATERIALS AND METHODS

Assembly of FAM–PNA–peptide conjugates with stable linkages

These were synthesized manually on a 5 μmol scale using a polyethylene syringe fitted with a 10 μm polyethyelene

frit (Isolute SPE Accessories) attached to a manifold multi-filtration device, and Fmoc chemistry (28). Fmoc-PAL-PEG-PS resin and Fmoc (Bhoc) PNA monomers were purchased from Applied Biosystems and used at 0.2 M dissolved in *N*-methylpyrollidone (NMP). The activator was 0.2 M PyAOP (or PyBOP) in DMF, and a mixture of DIPEA and 2,6-lutidine to give a 0.4 M solution in DMF was used as the base solution (reagent mix A). For conjugates **1**–**4** (Figure 2), after PNA assembly an Fmoc-AEEA spacer (O-linker, Applied Biosystems) was coupled followed by amino acid couplings, each carried out with 0.2 M PyBOP in DMF and 0.4M DIPEA (660 µl in 10 ml) in DMF (reagent mix B). For conjugates **5** and **6**, peptide synthesis was carried out before PNA synthesis and for conjugates **7** and **8**, peptide assembly was both before and after PNA assembly with spacers between each. Both PNA monomers and amino acid monomers were double coupled for 30 min per coupling. The resin was washed five times with DMF after each coupling. Fmoc deprotection was carried out with 20% piperidine in DMF (3 min, then 12 min) and resin washed again five times with DMF. 6-Carboxyfluorescein diacetate (6-CDFA; Sigma) (four equivalents relative to resin loading) was dissolved in a minimal volume of NMP and four equivalents of PyBOP dissolved in DMF added followed by four equivalents of DIPEA. The mixture was left for 10 min and another 4 equivalents of DIPEA added to the resin. After 16 h, the resin was washed thoroughly with DMF and deacetylated by treatment with 20% piperidine in DMF.

Assembly of $(K)_8$–PNA–K(FAM) (conjugate 9) and Cys(Npys)–PNA (towards conjugates 10–15)

These were synthesized on 5 µmol scale on an APEX 396 Robotic Peptide Synthesizer using the same reagents and resin as for manual synthesis. Fmoc deprotection was carried out with 20% piperidine in DMF (1 min, then 4 min), amino acid deprotection with 20% piperidine in DMF (3 min then 12 min). After five times washing with DMF, PNA was double coupled using reagent mix A and amino acids were double coupled using reagent mix B, each with a reaction time of 30 min per coupling. Boc-Cys(NPys) was used in the synthesis of PNAs required for disulfide coupling. Fmoc-Lys(Boc) was used for the $(Lys)_8$ sequence and Fmoc-Lys(Mmt) for the residue for fluorescent labelling. After washing five times with DMF, a capping step was carried out using 5% acetic anhydride, 6% 2,6-lutidine in DMF (2×5 min), followed by washing five times with DMF. The N-terminal Fmoc group needs to be removed (as above) before final cleavage.

In the case of $(Lys)_8$–PNA–Lys(Mmt), the resin was washed with DCM and the Mmt group removed by treatment with nine aliquots of 2% trifluoroacetic acid, 5% triisopropylsilane (TIS) in DCM (5 min incubation for every aliquot, 45 min in total). The resin was washed with 1× DCM and 1× DMF. To 6-CFDA (10 equivalents relative to resin loading) dissolved in a minimal volume of NMP was added HOAt (10 equivalents) dissolved in DMF and diisopropylcarbodiimide (DIC) (10 equivalents), premixed for 10 min, and reacted with the resin for at least 16 h at room temperature, the resin washed thoroughly and then deacetylated by treatment with 20% piperidine in DMF (as above).

Deprotection and purification of PNA

The resin was treated with 95% TFA, 2.5% H_2O, 2.5% TIS with addition of 10% phenol as scavenger for a minimum of 90 min. PNAs were analysed and purified by reversed phase high-performance liquid chromatography (HPLC) on a Phenomenex Jupiter C18 column (see below) with buffer A, 0.1% TFA in water; buffer B, 10% buffer A in acetonitrile and monitoring at 260 nm with a gradient of 10–50% B gradient over 30 min. MALDI-TOF mass spectrometry was carried out on a Voyager DE Pro BioSpectrometry workstation with a matrix of α-cyano-4-hydroxycinnamic acid, 10 mg ml^{-1} in acetonitrile-3% aqueous TFA (1:1, v/v). The accuracy of the mass measurement is regarded as ±0.05%.

Synthesis of Cys peptides

Tat-Cys, R_9F_2-Cys, Penetratin-Cys and R_6-Penetratin-Cys were purchased as C-terminal amides from Southampton Polypeptides. Transportan-Cys peptides were synthesized on a PerSeptive Biosystems Pioneer peptide synthesiser (100 µmol scale) using standard Fmoc/*tert*-butyl solid phase synthesis techniques as C-terminal amide peptides using NovaSyn TGR resin (Novabiochem). Deprotection of all peptides and cleavage from solid support was achieved by treatment with TFA in the presence of triethylsilane and water (each 3%). Purification was carried out by reversed phase HPLC as described previously (15) and MALDI-TOF mass spectrometry with the same matrix as for PNA.

Disulfide conjugates of Cys(NPys)–PNA with Cys-peptides (conjugates 10–15)

To an eppendorf tube containing the Npys-activated PNA oligomer (20 nmol in 25 µl water) was added 1 M NH_4Ac (pH 7, 10 µl) followed by the Cys-peptide to be conjugated (40 nmol, 4 µl of 10 mM stock solution). In the case of Transportan and derivatives, 50 µl of acetonitrile was added prior to peptide addition to prevent precipitation of the peptide at neutral pH. The solution was thoroughly mixed and allowed to stand for 30 min, whereupon the conjugate was purified in one aliquot by reversed phase HPLC using a Phenomenex Jupiter C18 column (5 µm, 300 Å, 250×4.6 mm^2) heated to 45°C: Flow rate 1.5 ml min^{-1}, Buffer A—0.1% TFA (aqueous), Buffer B—90% acetonitrile, 10% Buffer A. Gradient 5–30% B buffer in 25 min for Penetratin, R_9F_2, and R_6-Penetratin conjugates (**11**, **12** and **13**, respectively). A gradient of 5–50% B buffer was used for Transportan conjugates **14** and **15**. For conjugate 10, a step gradient was necessary because of close elution of conjugate, Tat and PNA: 5–10% B (2 min); 10–12.5% B (2 min); 12.5% B (4 min); 12.5–15% B (2 min); 15% B (4 min); 15–17.5% B (2 min); 17.5% B (4 min); 17.5–20% B (2 min); 20% B (4 min). The product was collected, lyophilized and analysed by MALDI-TOF mass spectrometry as described above for PNA alone. As an example, the HPLC purification profile for the R_6–PenC–PNA conjugate **13** (Supplementary Figure 1A), the HPLC analytical profile of the purified product (Supplementary Figure 1B) and mass spectrum (Supplementary Figure 2) are shown.

Inhibition of Tat-dependent *trans*-activation in cells

Inhibition of HIV-1 Tat-mediated *trans*-activation by CPP–PNA conjugates in HeLa cells (Figure 3) was carried out

similarly to that described previously (22,23). Briefly, in each experiment two identical 96-well plates were prepared with 10×10^3 HeLa Tet-Off/Tat/luc-f/luc-R cells per well and incubated at 37°C for 24 h. One of the plates was used for the luciferase assay and the other for the cytotoxicity assay. Conjugates were prepared at 2.5 μM concentration in Opti-MEM (Invitrogen), subsequently diluted and added to the cells for 6 or 24 h incubation, cells washed in phosphate-buffered saline (PBS) and followed by 18 h incubation in DMEM/10% fetal bovine serum (FBS). For chloroquine experiments (Figure 4), conjugates were prepared at 2.5 μM concentration and 100 μM chloroquine in Opti-MEM, subsequently diluted by 100 μM chloroquine in Opti-MEM and added to the cells for 6 h incubation, cells washed as before, followed by 18 h incubation in DMEM/10% FBS. For the time course study (Figure 5), incubations with conjugates and 100 μM chloroquine were carried out for 2, 4, 6 and 8 h, respectively, before treatment as above.

Luciferase assay. Cell lysates were prepared and analysed using the Dual Luciferase Reporter Assay System (Promega) and relative light units for both firefly and *Renilla* luciferase read sequentially using a Berthold Detection Systems Orion Microplate luminometer. Each data point was averaged over two replicates of three separate experiments.

Toxicity assay. The extent of toxicity was determined by measurement of the proportion of live cells colorimetrically using CellTiter 96 AQ_{ueous} One Solution Assay (Promega). The absorbance at 490 nm was read using a Molecular Devices Emax Microplate Reader.

Each data point was averaged over two replicates of three separate experiments. The relative light units in the luciferase assays were normalized to the absorbance data from the toxicity assay, which reflects the amount of live cells and then expressed as a percentage compared with the luciferase activities of HeLa cells treated in the absence of CPP–PNA. The error bars reflect the full range of the experimental values and are not SDs. It is common to normalize the firefly luciferase levels to that of the *Renilla* luciferase levels when co-transfection of plasmids is used. However in this stably integrated system, the level of *Renilla* luciferase is 20-fold lower than that of firefly luciferase and is thus much more sensitive to fluctuations resulting from small changes in cell growth conditions. Showing a simple ratio of the two levels unreasonably amplifies these fluctuations. We have therefore found it more beneficial to show the two sets of luciferase data separately (Figures 3 and 4) and to assess the extent of level changes or otherwise in each set.

Confocal microscopy

HeLa cells (15×10^3) were plated on an 8-well Lab-Tek chambered coverglass (Fisher Scientific) in DMEM/10%FBS and cultured overnight. The medium was discarded and cells were washed with PBS followed by incubation with 300 μl of 2.5 μM CPP–PNA conjugate or 2.5 μM CPP–PNA conjugate/100 μM chloroquine in OptiMEM for 5.5 h. For nuclear staining, 50 μl OptiMEM containing hydroethidine (50 μg ml^{-1}) was added to each well and incubated for 0.5 h at 37°C. After two washes, 200 μl of OptiMEM (without phenol red) (Invitrogen) medium containing HEPES buffer was added into the wells for observation of living cells.

The cells were observed with a Radiance 2100 confocal system on a Nikon Eclipse TE300 inverted microscope using a 60× Planapo objective N.A. 1.4.A 488 nm Argon laserline was used to excite fluorescein and a HQ 515/30 emission filter was used for observation of the green emission. Hydroethidine was excited with a 543 nm (green) HeNe laser and detected using a HQ 570LP (orange) emission filter. A dual fluorescence method was used with a differential interference contrast transmission channel. The images in the three channels were acquired sequentially at ~1 frame/s with a scanning resolution of 512 × 512 pixels and a Kalman average of 10 frames was used. When comparing the uptake or activity of the PNA conjugates the imaging conditions (such as photomultiplier gain/offset, laser intensities and confocal aperture size) were kept constant for the observation of the different conjugates, so that the intensities represent the true differences in uptake/activity.

RESULTS

In our earlier work, we reported that a 12mer PNA targeted to residues 24–35 of the apical loop of the HIV-1 TAR (Figure 1A) blocked Tat binding *in vitro* as well as Tat-dependent *in vitro* transcription in HeLa cell extract (21). More recently we have studied Tat-dependent *trans*-activation activity in HeLa cells and showed that a 16mer OMe/LNA steric block oligonucleotide was ~2-fold more inhibitory than a 12mer (22,23). Since Kaushik *et al*. (24) showed that a 16mer PNA targeted to TAR (residues 20–34) had several fold larger inhibitory activity than a 12mer PNA in reverse transcription, Tat-dependent *trans*-activation and HIV production assays, we have focussed our CPP–PNA conjugate studies on a similar 16mer PNA targeted to HIV-1 TAR (residues 21–35) (Figure 1A).

Our HeLa cell line carrying stably integrated luciferase reporters, used by us in several previous studies (22,23,29), has significant advantages for the study of the inhibition of Tat-dependent *trans*-activation activity (Figure 1B). In this 3-plasmid system, HIV-1 Tat is produced in *trans* to control production of GL3-firefly luciferase from the HIV-1 LTR, whilst a control *Renilla* luciferase is under constitutive CMV promoter direction. In contrast to the transient plasmid reporter system of Kaushik *et al*. (24), in order to see significant steric block inhibition of the TAR RNA system, oligonucleotides or PNA must be delivered efficiently to the nucleus of almost all cells, since each cell contains the three plasmids. The integrated plasmid system would be expected to mimic more closely an integrated HIV-1 provirus than transient transfection. Since unconjugated PNA is not taken up by cells, conjugation with a CPP, minimally a few Lys residues (17), is essential to achieve at least some cell binding and entry. We wished to determine how the nature of the CPP and the way it is linked to the PNA influences the ability of the PNA component to enter the cell, reach the nucleus and inhibit Tat-dependent *trans*-activation.

Synthesis of stably-linked and disulfide-linked conjugates of CPPs to 16mer PNA

A series of stably-linked CPP–PNA conjugates was synthesized using the Fmoc method (28), where the linkage between

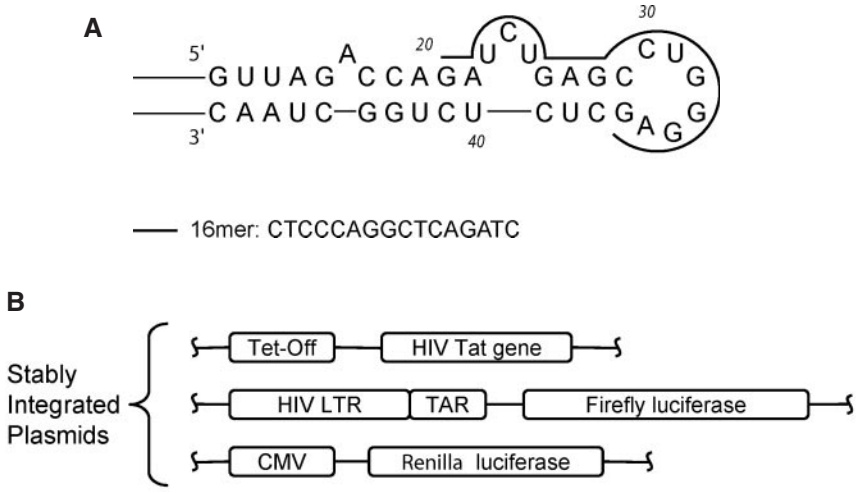

Figure 1. (**A**) Secondary structure of the TAR RNA apical stem–loop, the binding site on TAR and sequence of the PNA 16mer. (**B**) Stably integrated plasmids within the HeLa Tet-Off/Tat/luc-f/luc-R cell line used for *trans*-activation inhibition studies.

the PNA and peptide parts consisted of a short polyether linkage (AEEA, 8-amino-3,5-dioxo-octanoic acid, also known as an O-linker) (Figure 2A, conjugates **1**–**8**). All conjugates were purified by reversed phase HPLC and characterized by MALDI-TOF mass spectrometry. CPPs used were either the Tat peptide (residues 48–58) (30), an SV40 nuclear localization signal (NLS) (31,32), Transportan (25) or a shorter 21mer version of Transportan [known as TP10 or Transportan 21 (33)]. In conjugates **1**–**4**, a single CPP (Tat, Transportan, TP10 or NLS, respectively) was linked to the N-terminus of the 16mer PNA, spaced by an O-linker (Figure 2A). In conjugates **5** and **6**, a single CPP (TP10 or NLS) was linked to the C-terminus of the PNA, spaced by an O-linker. In conjugates **7** and **8**, both NLS and Tat CPPs were added, one on each end in different order, each spaced by an O-linker. A carboxyfluorescein (FAM) label was coupled to the N-terminus of each conjugate to enable cell fluorescence uptake studies.

A different type of stably-linked CPP–16mer PNA conjugate was also synthesized that carried eight lysine residues on the N-terminus [Figure 2A, conjugate **9**]. Conjugate **9** was prompted by the work of Siwkowski *et al*. (34) who showed that a K_8–PNA construct was very effective at redirection of splicing of a CD40 mRNA when added to BCL_1 or macrophage cells, and that this was due to enhanced cell uptake resultant from the use of the K_8 conjugate acting effectively as a CPP. In conjugate **9**, the FAM label was attached to the PNA moiety on the C-terminus via the ε-amino group of a single K residue.

In order to compare with the Transportan-PNA conjugate of Kaushik *et al*., (26) which utilized a disulfide linkage, we synthesized a range of CPP–PNA conjugates that contained a disulfide linkage (Figure 2B). These were synthesized by conjugation of Cys–peptides with Cys–PNA activated with a nitropyridylsulfenyl (NPys) group, purified by reversed phase HPLC and characterized by MALDI-TOF mass spectrometry. Six such conjugates were prepared (Figure 2B) from PNA 16mer containing three C-terminal K residues and as CPPs either Tat (30), Penetratin (35), R_9F_2 (36), Transportan or a novel R_6-Penetratin chimeric peptide that we have described recently (15). In four cases (**10–13**) the Cys residue was located on the C-terminus of the peptide, in one case Transportan was placed at the N-terminus (**14**) [which is similar to that described previously by Kaushik *et al*. (26)], and in the case of construct **15**, a Cys residue replaced K-13 in Transportan.

Inhibition of Tat-dependent *trans*-activation by CPP–PNA

We tested the ability of CPP–PNA constructs to inhibit Tat-dependent *trans*-activation by incubation with HeLa Tet-Off/Tat/luc-f/luc-R cells (21,23) for 6 or 24 h in the absence of any transfection agent. Cells were then washed and subsequently grown for 18 h. Firefly luciferase activity results from HIV-1 Tat-dependent transcription, whilst *Renilla* luciferase activity acts as an internal control to check that there is no inhibition of general transcription/translation.

In the case of stably-linked conjugates **1**–**9**, there was no significant reduction seen either of firefly luciferase or *Renilla* luciferase expression up to 2.5 μM tested (data not shown). We then tested the six disulfide-linked CPP–PNA conjugates. Tat, Penetratin and R_9F_2 conjugates **10**–**12** showed no activity up to 2.5 μM tested (data not shown). For 6 h incubation (Figure 3A, upper panel), the R_6-Penetratin disulfide conjugate **13** showed no activity, but both Transportan disulfide conjugates **14** and **15** showed a small dose-dependent reduction of firefly luciferase activity (Figure 3A, upper panel). The *Renilla* luciferase activity did not drop significantly over the same concentration range (Figure 3A, lower panel). Note that the absolute level of *Renilla* luciferase activity in terms of light units is only 5–10% of that of the firefly luciferase in this cell line. Sporadic increases in *Renilla* luciferase fluorescence for particular constructs are occasionally observed, e.g. construct **14**, reflecting the much higher sensitivity of the *Renilla* luciferase to additives or cell growth conditions compared with firefly luciferase. A significant reduction in *Renilla* luciferase expression would have been expected had there been any non-specific transcription/translation suppressive effect upon addition of the CPP–PNA, which is clearly not the case. Cell viability for 6 h incubation with the highest concentration

A. Stably-linked conjugates

Conjugate	Description	Calculated molecular mass	Observed MALDI molecular mass
1	FAM-Tat-*O*-PNA-$CONH_2$	6253.06	6254.49
2	FAM-TP-*O*-PNA-$CONH_2$	7598.75	7603.61
3	FAM-TP10-*O*-PNA-$CONH_2$	6941.04	6945.60
4	FAM-SV40 NLS-*O*-PNA-$CONH_2$	5642.42	5644.12
5	FAM-PNA-*O*-TP10-$CONH_2$	6941.04	6945.24
6	FAM-PNA-*O*-SV40 NLS-$CONH_2$	5642.42	5643.52
7	FAM-SV40 NLS-*O*-PNA-*O*-Tat-$CONH_2$	7263.36	7262.32
8	FAM-Tat-*O*-PNA-*O*- SV40 NLS-$CONH_2$	7263.36	7263.50
9	NH_2-K_8-PNA-K(FAM)-$CONH_2$	5785.69	5791.78

FAM = Carboxyfluorescein label
O = -NH-$(CH_2CH_2O)_2CH_2CO$-
Tat = GRKKRRQRRRP
TP = GWTLNSAGYLLGKINLKALAALAKKIL
TP10 = AGYLLGKINLKALAALAKKIL
SV40 NLS = PKKKRKV

B. Disulfide-linked conjugates

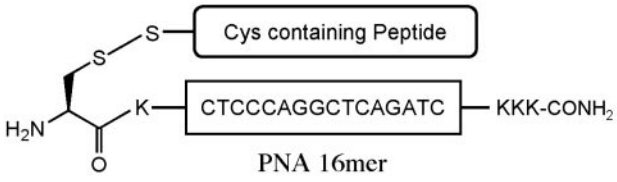

Conjugate	Peptide[a]	Calculated molecular mass	Observed MALDI molecular mass
10	Tat-**C**	6483.88	6486.43
11	Pen-**C**	7350.95	7355.68
12	R_9F_2-**C**	6708.22	6711.56
13	R_6Pen-**C**	8288.07	8288.17
14	**C**-TP	7831.56	7836.82
15	TP(int **C**)[b]	7703.38	7704.88

[a] **C** denotes where disulfide linkage is
[b] Internal **C** replaces K 13 in Transportan (TP) i.e. GWTLNSAGYLLG-**C**-INLKALAALAKKIL
Pen = RQIKIWFQNRRMKWKKGG

Figure 2. (**A**) Structures of various FAM-labelled stably-linked CPP–PNA and PNA–CPP conjugates **1–9** and their calculated and observed mass values. (**B**) Structure of various disulfide-linked CPP–PNA conjugates **10–15** and their calculated and observed mass values. The linkage is in all cases between an N-terminal Cys residue on the PNA and a Cys residue within the peptide either on the C-terminus (**10–13**) N-terminus (**14**) or an internal residue (**15**). These conjugates do not carry a FAM label.

(2.5 μM) of the stably-linked CPP–PNA was >95% in all cases and for disulfide-linked conjugates was >90%.

For 24 h delivery of the CPP–PNAs, a strong dose-dependent reduction of firefly luciferase activity was seen for all three conjugates **13–15** (Figure 3B, upper panel), whilst no significant reduction in *Renilla* luciferase activity was seen in any case (Figure 3B, lower panel, note that in this case there was no significant sporadic increase for the same conjugate **14**). Thus the R_6-Penetratin and the two Transportan conjugates of PNA 16mer, in contrast to Tat, Penetratin and R_9F_2 conjugates, must in some way assist significant amounts of PNA to reach the nucleus and interact with TAR RNA during the extended time 24 h time period in order to show such strong inhibition of Tat-dependent *trans*-activation.

Effect of chloroquine addition on CPP–PNA conjugates

In common with most types of biomolecules, it is well known that oligonucleotides and their analogues enter most cells via an endocytotic pathway, of which there are many types (37). In our previous studies with CPP conjugates of LNA/OMe oligonucleotides, confocal microscopy evidence was obtained that the most probable limiting factor in obtaining *trans*-activation inhibition was sequestration within endosomal or other membrane-bound cytosolic compartments (15). We

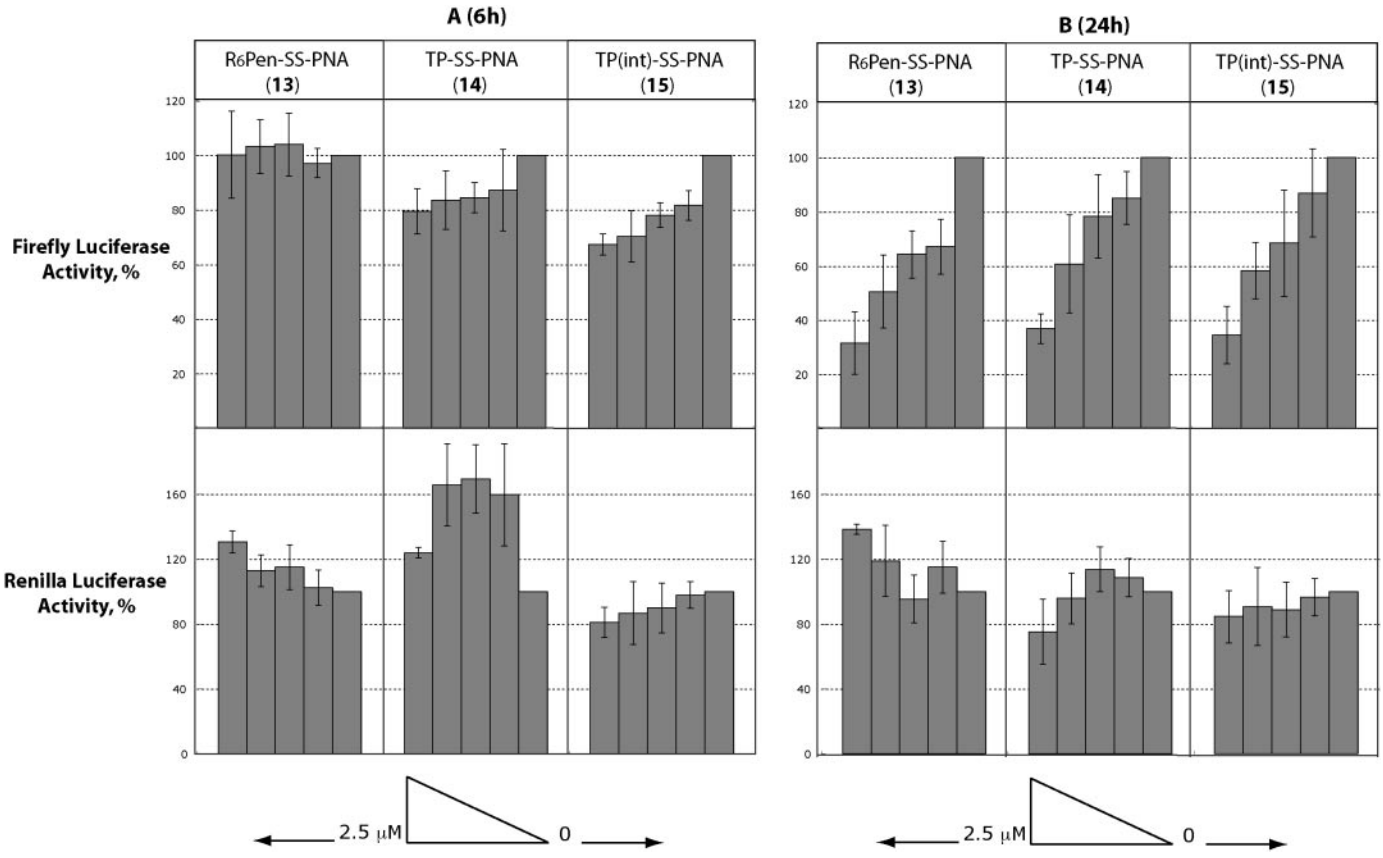

Figure 3. *Trans*-activation inhibitory effects of disulfide-linked CPP–PNA conjugates **13**–**15** in the HeLa cell reporter assay with 6 h delivery (**A**) or 24 h (**B**). Firefly luciferase activity represents Tat-TAR dependent expression whilst *Renilla* luciferase activity represents control constitutive expression. Bars (left to right) in each case represent 2.5, 1.25, 0.625, 0.312 and 0 μM CPP–PNA concentrations.

therefore asked if addition of a known lysosomotropic reagent could enhance the release of CPP–PNA conjugates from such compartments. Chloroquine is an anti-malarial drug and a weak base that passes through membranes in its unprotonated form and accumulates in acidic compartments, such as lysosomes and endosomes, where it leads to osmotic swelling (38). The reagent has been used to study endosomal uptake of antisense oligodeoxynucleotides (1,39,40). The reagent is thought to promote the disruption of endosomal compartments. Similarly lysosomotropic agents increase the efficiency of transgene expression by non-viral delivery vectors (41,42).

We therefore carried out the *trans*-activation inhibition assay with the HeLa cell reporter system with addition of CPP–PNA for 6 h in the presence of 100 μM chloroquine, cells washed and grown for a further 18 h. For stably-linked Tat-PNA conjugate (**1**), there was now seen a significant level of reduction of firefly luciferase (Figure 4A). A smaller reduction (reduction most noticeable at the highest CPP–PNA concentration used) was seen for Transportan-PNA (**2**), TP10–PNA (**3**), NLS–PNA–Tat (**7**) (Figure 4A) and also for PNA–TP10 (**5**) and Tat–PNA–NLS (**8**) (data not shown). No inhibitory activity was observed for NLS–PNA (**4**) or PNA–NLS (**6**) or for K_8–PNA (**9**) (data not shown). No reduction was seen of *Renilla* luciferase activity in any case (data not shown). Cell viability was >85% for all stably-linked CPP–PNAs in the presence of chloroquine.

The three CPP–PNA disulfide conjugates (**13–15**) that had previously shown high firefly luciferase inhibition activity at 24 h in the absence of chloroquine (Figure 3B) showed a strong dose-dependent inhibition of firefly luciferase expression when chloroquine was co-administered with the CPP–PNA for 6 h (Figure 4B). No reduction was seen in any case in *Renilla* luciferase expression as conjugate concentration was increased (data not shown). A small increase in *Renilla* luciferase activity was again seen at high CPP–PNA concentration in occasional cases (data not shown). Cell viability was >70% for the disulfide-linked conjugates in the presence of chloroquine.

To show that sequence-specificity is maintained when chloroquine is co-administered, we tested controls of R_6-Pen-S-S-PNA (**13**) with scrambled and mismatched PNA sequences and both of these showed no inhibitory activity of firefly luciferase expression (Figure 4B). Similar scrambled and mismatched controls for Transportan disulfide PNA conjugate **14** were also inactive (data not shown). Thus chloroquine addition has no effect on the sequence-specificity of the inhibition of Tat-dependent *trans*-activation of the active CPP–PNAs. No effect was seen of 100 μM chloroquine on HeLa cell viability (data not shown) and the level of firefly luciferase activity was not significantly affected by chloroquine alone (Figure 4A and B, minus chloroquine control). However, chloroquine alone treatment did show a reduction

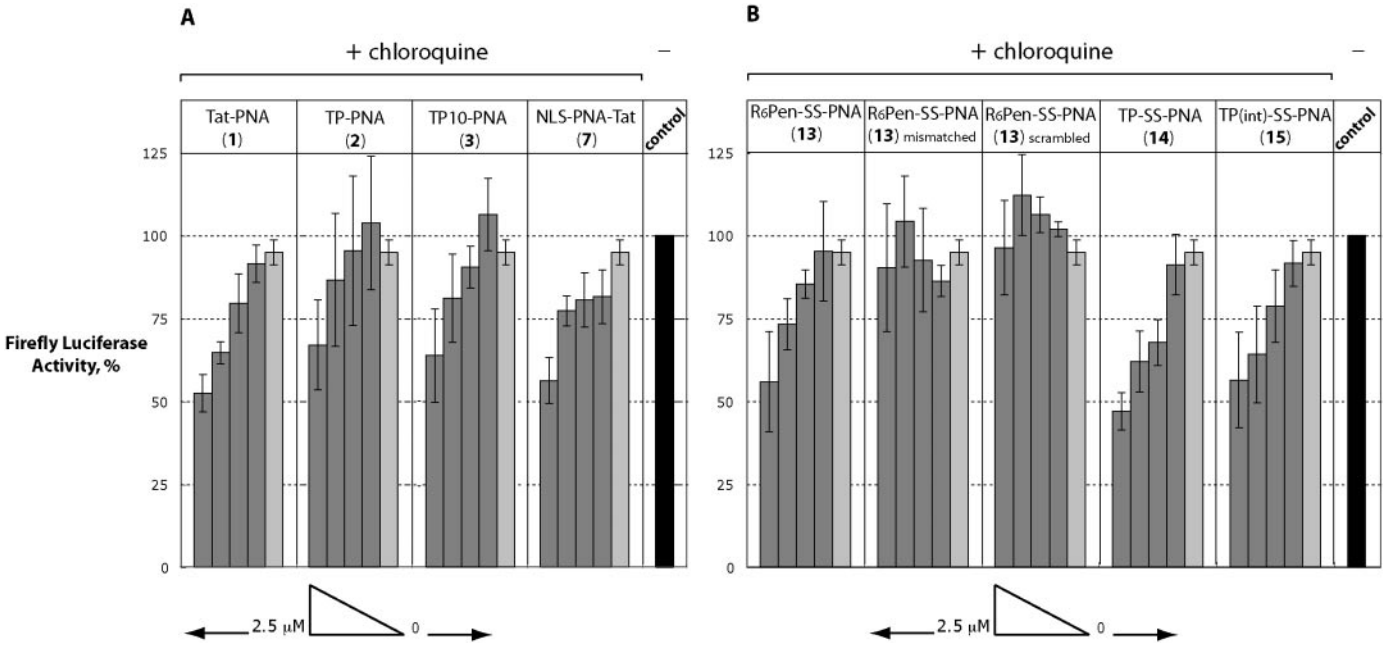

Figure 4. *Trans*-activation inhibitory effects (firefly luciferase activity) of CPP–PNA conjugates in the HeLa cell reporter assay with delivery for 6 h in the presence of 100 μM chloroquine. (**A**) Stably-linked conjugates Tat–PNA (**1**), TP–PNA (**2**), TP10–PNA (**3**) and NLS–PNA–Tat (**7**). (**B**) Disulfide-linked conjugates R_6–Pen-S-S–PNA (**13**), mismatched conjugate **13** (PNA sequence, CTCCGCAGCTCAGATC), scrambled conjugate **13** (PNA sequence, ATCGCTCGCACCATGC), TP–S-S–PNA (**14**) and TP(int)–S-S–PNA (**15**). Bars (left to right) in each case represent 2.5, 1.25, 0.625, 0.312 and 0 μM (light shaded bar) CPP–PNA concentrations. Control (black bar), absence of CPP–PNA and absence of chloroquine.

in the level of *Renilla* luciferase (but no further reduction when CPP–PNA was added) (data not shown).

Overall the chloroquine co-administration data are consistent with the hypothesis that release from endosomal or membrane-bound compartments is limiting in attaining *trans*-activation inhibition activity for CPP–PNA conjugates. Since some stably-linked CPP–PNAs gained activity when chloroquine was co-administered (Figure 4A), a cleavable disulfide bond between CPP and PNA is clearly not essential. However, there is not as yet a fully consistent structure–activity relationship, since no significant inhibition of firefly luciferase was seen with co-administration of chloroquine with Tat-S-S-PNA, Penetratin–S-S–PNA and R_9F_2–S-S–PNA disulfide conjugates **10**–**12** for 6 h (data not shown), which were also inactive in the absence of chloroquine (data not shown).

To look at the time course for the effect of chloroquine on nuclear Tat-dependent *trans*-activation inhibition activity, we co-incubated 2.5 μM of the most active stably-linked conjugate, Tat-PNA (**1**), with 100 μM chloroquine for different times, washed the cells and continued growth in each case for 18 h. The results showed that the majority of the inhibitory effect is seen within 6 h with very little additional reduction in firefly luciferase activity after 8 h (Figure 5). Similar time courses were seen for lower concentrations of Tat-PNA, with correspondingly smaller firefly luciferase expression reductions (data not shown). This shows that 6 h co-administration, the time point when the set of data in Figure 4 was taken, was reasonably well chosen to see most of any observable *trans*-activation inhibition enhancement effect.

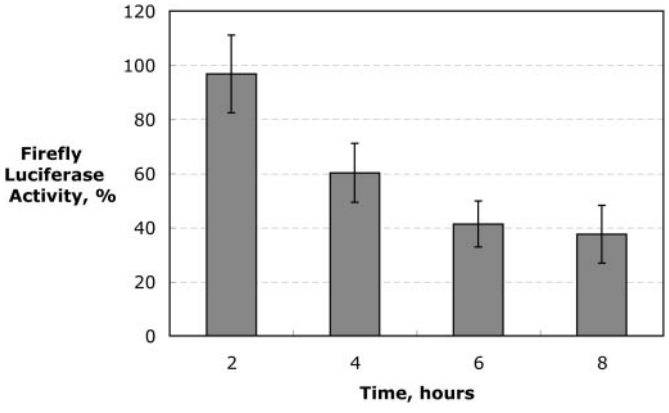

Figure 5. *Trans*-activation inhibitory effects (firefly luciferase activity) of 2.5 μM Tat-PNA (**1**) incubated for 2, 4, 6 or 8 h, respectively, with HeLa reporter cells, cells washed and grown for 18 h before assay.

Confocal microscopy of FAM-labelled CPP–PNA in the absence and presence of chloroquine

To obtain visual evidence for chloroquine release from endosomal or membrane-bound compartments, we examined by live-cell confocal microscopy the ability of FAM-labelled constructs to enter the HeLa cells after 5.5 h, a similar time to that used for the activity experiments (Figure 6). A hydroethidine dye was used to stain the cell nucleus, which makes it easier to observe any nuclear uptake (green colour or yellow colour when overlayed), but also only the nuclei of live cells are stained red, ensuring that only healthy cells are included

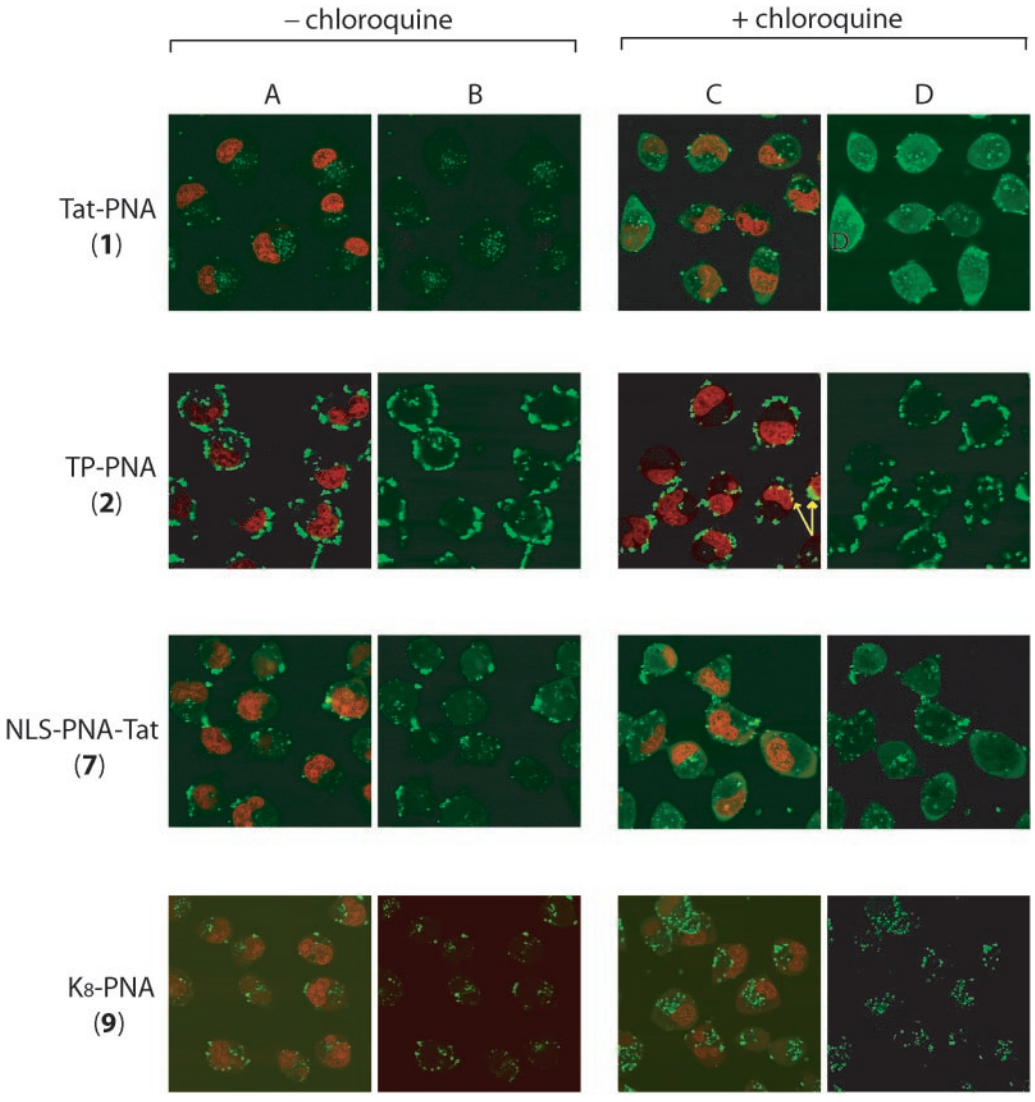

Figure 6. Confocal microscopy images of the uptake of fluorescein (FAM)-labelled CPP–PNA conjugates when incubated for 5.5 h with unfixed HeLa cells. Nuclei are stained red with hydroethidine. (**A** and **C**) Orange filter to view both the red colour of hydroethidine and the fluorescein fluorescence. (**B** and **D**) Green filter to view only the fluorescein fluorescence. (A and B) Show incubations in the absence of chloroquine, (C and D) Show incubations in the presence of 100 μM chloroquine. First line Tat–PNA (**1**); second line Transportan–PNA (**2**); third line NLS–PNA–Tat (**7**); fourth line K_8–PNA (**9**). In (C), second line, yellow dots are marked with arrows showing co-localization of hydroethidine dye and fluorescein fluorescence on the inner wall of the nucleus in several nuclei.

in observations (Figure 6A and C, orange filter). Figure 6B and D shows green emission only. Note that all confocal microscopy experiments used live cells that are unfixed and which are not subject to artefacts of cell fixation (43).

All FAM-labelled CPP–PNA constructs **1**–**9** showed significant cell uptake. For example in the absence of chloroquine, Tat-PNA (**1**) showed a punctate distribution of fluorescence in the cytosol with rather small puncta that were quite well distributed and typical of endosomal sequestration (Figure 6A and B, first line). In contrast Transportan–PNA conjugate (**2**) (Figure 6A and B, second line) and TP10–PNA (**3**) (data not shown) showed strong uptake but a quite different distribution, being concentrated either at or close to the cell surface in large aggregates, with just a few large puncta seen within the cytosol. FAM-labelled constructs containing both NLS and Tat peptides showed a punctate distribution more akin to that of Tat–PNA. For example NLS–PNA–Tat (conjugate **7**, Figure 6A and B, third line) showed both small and large cytosolic puncta. The K_8-PNA uptake pattern (conjugate **9**) (Figure 6A and B, fourth line) looked very similar to that of Tat–PNA conjugate **1**. Since the FAM label in the case of K_8–PNA is on the C-terminus of the PNA (compared with the N-terminus of the peptide in the case of Tat–PNA), this gives confidence that any fluorescence seen is due to intact CPP–PNAs during the 5.5 h delivery period and not as a result of FAM label release. The lack of significant nuclear fluorescence seen in all four conjugate cases is consistent with the lack of activity of the stably-linked CPP conjugate constructs in the *trans*-activation inhibition assay in the absence of chloroquine.

Confocal microscopy of HeLa cells treated for 5.5 h with FAM-labelled Tat–PNA in the presence of 100 μM chloroquine was informative. Conjugate **1** (Figure 6C and D, first line) showed in addition to punctate structures in the cytosol,

a significant and uniform fluorescence in the cytosol and nucleus. This is particularly apparent in the image taken with green emission (Figure 6D), where the hydroethidine red colour is not visible. In contrast, Transportan–PNA (conjugate **2**) in the presence of chloroquine showed the majority of the fluorescence as large aggregates at or close to the cell surface (Figure 6C and D, second line), similar to that seen in the absence of chloroquine (Figure 6A and B). However with hydroethidine staining (Figure 6C) some of the nuclei showed yellow spots (owing to overlay of red and green) just inside the nuclear membrane (yellow arrows). There was very little green fluorescence seen in the cytosol under the green emission (Figure 6D). This suggests that the Transportan–PNA conjugate **2** may have quite different characteristics of cell uptake and trafficking.

NLS–PNA–Tat (**7**) (Figure 6C and D) showed general fluorescence release very similar to that of Tat–PNA (**1**), but less strongly. The same result was seen for Tat–PNA–NLS (**8**) (data not shown). Other constructs such as K_8–PNA (**9**) (Figure 6C and D) did not show strong evidence of uniform cell fluorescence when chloroquine was co-administered and the fluorescence remained punctate, similar to that in the absence of chloroquine (Figure 6A and B). The overall fluorescence in the cytosol (either in endosomes or general) appeared to be higher in many cases when chloroquine was used, but one should note that the overall levels of fluorescence cannot be directly compared in the presence and absence of chloroquine, because fluorescein has substantially reduced fluorescence at the low pH value found within endosomes and chloroquine itself (being a base) is also likely to affect pH.

Overall, the confocal microscopy results show that the nature of the CPP attached stably to the PNA by O-linker affected both the type of vesicular structure seen in the cytosol (mostly punctate or mostly aggregates at the cell surface) as well as whether and how the fluorescence is released by chloroquine addition. It is clear that basic peptides such as Tat promote a radically different cell uptake pattern of PNA (conjugate **1**) from that of Transportan (conjugate **2**). In general, confocal microscopy data provides additional evidence for sequestration of CPP–PNA in endosomal or membrane-bound compartments.

DISCUSSION

The importance of this study centres on how the type of CPP and the way it is linked to a PNA 16mer directed against a HIV-1 TAR target affects the ability of PNA to inhibit Tat-dependent *trans*-activation in HeLa cell nuclei using our stably integrated, double-luciferase reporter plasmid system. The TAR apical stem–loop is a well-validated, steric block antisense target by us (15,22,23,29) and by others (24,44,45). Dose-dependence and sequence-specificity in cells was established previously using lipid-delivered oligonucleotide analogues. Inhibition at the RNA level was verified using a Tat-dependent transcription assay with HeLa cell nuclear extract (22,23). In the current study, we found that two disulfide-linked conjugates of 16mer anti-TAR PNA to Transportan (linked in different ways) or a novel R_6-Penetratin chimeric peptide (conjugates **13**–**15**) were able to inhibit intracellular *trans*-activation at a significant level when incubated for 24 h (Figure 3). In contrast, PNA conjugates disulfide-linked to Tat, Penetratin and R_9F_2 (**10–12**) and a range of CPP conjugates having stable O-linkers between CPP and PNA components (**1–9**) were unable to elicit *trans*-activation inhibition (data not shown).

We have used co-administration of the lysosomotropic reagent chloroquine to provide strong evidence that the barrier to high *trans*-activation inhibition activity in the nucleus is poor release from endosomes or other membrane-bound compartments. The three disulfide-linked CPP–PNA conjugates **13**–**15** that showed inhibition on their own when incubated with cells for 24 h also showed substantial activity within 6 h in the presence of chloroquine, and the sequence-specificity of the inhibitory activity was maintained (Figure 4B). Some stably-linked conjugates that were inactive when delivered alone, e.g. Tat–PNA conjugate **1**, were able to gain significant inhibitory activity in the presence of chloroquine (Figure 4A). The time course of the *trans*-activation inhibitory activity showed that most of the effect occurred within 6 h (Figure 5). Thus an unstable disulfide linkage is not a prerequisite for activity if endosomal release can be enhanced by chloroquine. Surprisingly, activity was not enhanced significantly for some other conjugates, notably PNA disulfide-linked to Tat, Penetratin and R_9F_2 (conjugates **10**–**12**, data not shown). This shows that the structure–function relationship of inhibition activity and chloroquine enhancement is complex and not just a matter of cleavable versus stable linkage. Clearly though, disulfide-linked CPP–PNA **13**–**15** were the only ones that worked in the absence of chloroquine.

Folini *et al*. (46) described recently a photochemical approach to trigger endosomal release from adenocarcinoma cells DU145 of a naked PNA targeted to hTERT mRNA. Incubation of 18 h with high PNA concentration (10 μM) and a photosensitizer was used followed by a 60–80 s fluorescent light treatment. A significant reduction in telomerase activity was observed in cell extracts and some microscopy evidence was obtained for fluorescent PNA redistribution into cytosol and nucleus from endosomal vesicles. A stably-linked Tat–PNA was only slightly active at 2 μM when incubated for 48 h but these authors did not test photochemical release of Tat–PNA (46). Whilst consistent with Folini *et al*. (46), our data is important in that we have used CPP–PNAs, which have much better cell uptake and therefore can be used at lower concentration, short delivery periods (6 h) and a definite nuclear target (hTERT mRNA could have been inhibited either in cytosol or nucleus), as well as a known drug, chloroquine, to demonstrate endosomal release is limiting in attaining *trans*-activation inhibition in HeLa cells.

We observed endosomal and/or membrane sequestration for several stably-linked FAM-labelled CPP–PNA tested (Figure 6). This is consistent with previous observations by others in several cell lines for fluorescently labelled Tat–PNA and Penetratin–PNA, whereas no uptake was observed for PNA alone (4). The very different confocal microscopy uptake patterns of Tat–PNA (**1**) and Transportan–PNA (**2**) confirm previous suggestions that there are at least two classes of CPP, one broadly encompassed by Arg-rich domains, such as Tat (47) and our novel chimeric peptide R_6-Penetratin (15), and another by the more hydrophobic peptide Transportan (25,26,48). We found clear evidence for conjugate release from endosomes by confocal microscopy in the cases of

FAM-labelled stably-linked Tat–PNA (**1**) and NLS–PNA–Tat (**7**) (Figure 6). There was also some evidence of release into the nucleus for stably-linked Transportan–PNA (**2**). In this case there was no general cytosolic fluorescence but instead a different localization pattern that suggests an alternative trafficking pathway for Transportan–PNA.

Our experiments here do not address directly the issue of the type of uptake pathway(s) for the two types of CPP–PNA conjugate nor the precise role of chloroquine in facilitating activity and nuclear delivery. The punctate endosomal location of Tat–PNA **1**, the fluorescence release (Figure 6) and the gain of *trans*-activation inhibition activity (Figure 4) are all completely consistent with our previous data on Tat peptide and Tat–PNA showing sequestration in acidic endosomal compartments (43). In contrast, Transportan clearly directs the PNA into membrane-bound vesicular compartments that are different to those of Tat–PNA conjugates (compare conjugates **1** and **2** in Figure 6). Recently published studies with several cell lines using FACS analysis concluded that a TAMRA-labelled disulfide-linked Transportan–PNA was not taken up by a receptor-mediated or endocytotic process because the kinetics of uptake were not affected by low temperature or by the addition of phenylarsine oxide (27). Our results on chloroquine enhancement of *trans*-activation activity of two types of disulfide-linked TP–PNAs (**13** and **14**, Figure 4B) suggest that some sort of endosomal routing may nevertheless occur, at least in part. However, the clearly different pattern of uptake seen for stably-linked TP–PNA (**2**) in the absence and presence of chloroquine to that of Tat–PNA (**1**) and other cationic peptides (Figure 6) implies that a non-endocytic pathway of delivery is possible in the case of TP–PNA. Further comparative data between the two types of conjugate using specific classes of endocytosis inhibitor, as well as other cell trafficking analysis techniques, will be required to address this point with sufficient clarity.

We found that minimal CPPs, such as a stably-linked K_8–PNA conjugate **9** which was FAM-labelled at the C-terminus of the PNA, were not active in our assay up to 2.5 μM tested, even in the presence of chloroquine (data not shown). Nor did we see evidence for cytosolic release (Figure 6, fourth line). The fact that similar punctate fluorescence patterns were observed in the absence of chloroquine for both N-terminal FAM-labelled Tat–PNA and C-terminally labelled K_8–PNA (Figure 6, compare first and fourth lines) suggests that the fluorescence observed reflects intact CPP–PNA conjugate. It should be noted that biotin labelled Tat, Penetratin and R_9 peptides internalized in cells for several hours and rapidly isolated from cells without chance of proteolysis during isolation were found to be predominantly intact (49).

In work carried out in parallel using a K_8–PNA construct directed to a splice site to redirect splicing and up-regulate production of luciferase, chloroquine co-treatment allowed partial splicing correction and increased luciferase expression in keeping with partial release of the conjugate entrapped within endosomal compartments (50). Treatment with sucrose (which is also believed to promote endocytic vesicles swelling and destabilization) gave similar data. We believe that the splicing correction assay is probably much more sensitive than the anti-TAR *trans*-activation inhibition assay described here. We note that in a different splicing assay IC_{50}s for similar K_n–PNA conjugates were in the micromolar range (34).

Our work complements well previous studies using a disulfide-linked Transportan–PNA conjugate which was shown to inhibit HIV-1 production in chronically infected H9 cells (IC_{50} of 1 μM) when treated in culture for 6 h (26). In our Tat-dependent *trans*-activation assay, two different disulfide-linked Transportan–PNA conjugates and also an R_6–Penetratin–PNA conjugate showed similar inhibition levels (IC_{50} of 0.5–1 μM) (Figure 3) but in each case strong inhibition was only seen after 24 h delivery. Our evidence suggests that CPP–PNA conjugates are sequestered in endosomal or membrane-bound compartments and thus only slowly released. For further studies, we are currently constructing disulfide-linked PNA–peptide conjugates fluorescently labelled on the N-terminus of the PNA. Preliminary confocal microscopy studies on a Tat conjugate showed punctate endosomal sequestration similar to the stably-linked conjugates **1** and **9** (A.A. Arzumanov, unpublished data).

Our studies are important also in consideration as to what extent antiviral effects of PNA-peptides might be due to inhibition of Tat-dependent *trans*-activation. Chaubey *et al.* (27) found recently that their disulfide-linked Transportan–PNA conjugate was active with IC_{50} of 500 nM in an HIV infection inhibition assay when HIV-1 was used to infect CEM cells in the presence of conjugate. Because these experiments were carried out by co-incubation of virus and conjugate with cells, antiviral activity could arise for several reasons, such as interference with viral uptake, inhibition of reverse transcription within partially uncoated virions within the cytosol of infected cells, or by inhibition of Tat-dependent *trans*-activation once the proviral DNA has been integrated into the host. Blocking of reverse transcription *in vitro* by steric block oligonucleotides and PNA complementary to TAR has been well known for some years (51,52) but to what extent this can occur within cells is currently unclear. Our results show that blocking Tat-dependent *trans*-activation is a possible activity in cells, as evidenced by our robust integrated plasmid assay, and that this can be effected by two types of disulfide-linked TP–PNA and a new R_6–Penetratin–PNA. However, this cell activity was only obtained strongly after 24 h incubation.

Our results suggest that entrapment within endosomal or membrane compartments is probable to limit the antiviral activities of many PNA–peptide conjugates and thus there would now be great benefit in investigation of a much wider CPP range that might further enhance endosomal or membrane release. For example, our disulfide-linked R_6–Penetratin–PNA conjugate clearly belongs to a different class to Transportan–PNA conjugates. This peptide is a chimera between Penetratin and a short poly-Arg sequence (53), which is thought to act similarly to Tat peptide. This chimera is therefore a double CPP. We hope to extend our studies to antiviral activities of this and other similar CPP–PNA conjugates in the future.

Chaubey *et al.* (27) also showed that their TP–PNA conjugate was much more highly effective as a virucidal agent with a dose median of 66 nM when HIV-1 virions were pretreated with conjugate before infection of cells. This activity cannot be due therefore to *trans*-activation inhibition. The conjugate was shown to cause abortive termination of reverse transcription within virions, but only when treated at the much higher dose of 0.5 or 1.0 μM. Thus it is not

yet clear if the conjugate binds also to the viral envelope to prevent cell attachment or entry. Further, during preparation of this manuscript, Tripathi *et al*. (54) reported synthesis of Transportan, Transportan TP10 and C-terminally truncated Transportan-linked through a Cys residue added to ε-amino group of Lys-13, as well as Penetratin and Tat peptides linked through their N-termini, in each case to the N-terminus of fluorescein-labelled 16mer PNA. Interestingly, the HIV-1 virucidal activities all fell within a narrow range (28–72 nM dose median) with the Penetratin conjugate being the best, whilst antiviral activities varied from 400 nM IC_{50} for full-length Transportan conjugate to 1.1 μM for truncated Transportan conjugates. Penetratin and Tat conjugates showed 800 and 720 nM IC_{50} respectively. There was no clear correlation of the level of cell uptake as measured by FACS analysis with antiviral activity, and no cell localization experiments were reported.

Contrary to the observations of Tripathi *et al*. (54), who suggested that all these disulfide-linked conjugates are taken up by cells by similar non-endocytotic pathways, because uptake was not seen to be inhibited at 4°C, our confocal microscopy data (Figure 6) suggest sequestration of CPP–PNA in endosomal or membrane-bound compartments and release in the presence of the lysosomotropic reagent chloroquine. Clearly our *trans*-activation inhibition data (Figures 3 and 4) show that two classes of CPP (Transportan and R_6–Penetratin) disulfide-linked to PNA enable nuclear activity to be attained. No clear literature data are available as to whether intracellular cleavage of their disulfide linkages occurs or if PNA–peptide conjugates are released intact from the endosome or other membrane-bound compartment. Confocal microscopy studies of disulfide-linked conjugates carrying different fluorophores on PNA and peptide parts (32) may help to address this issue. But our important data show that a cleavable bond is not essential in principle since stably-linked Tat–PNA **1** is strongly active when chloroquine is co-administered (Figure 4B).

Whilst this manuscript was undergoing review, a paper was published showing that 6 mM calcium ions or 60–120 μM chloroquine co-administration increased the ability of stably-linked Tat-*O*-PNA or R_7–PNA to correct mis-splicing of luciferase mRNA 44- and 8-fold, respectively, in the nucleus of HeLa pLuc 705 cells, but no effect was observed for naked PNA (55). Evidence was presented that the mechanism involves endosomal release. The results presented are fully consistent with our data.

The TAR apical stem–loop target is highly sequence-conserved and is one of several potential targets in the HIV-1 RNA leader suitable for development of oligonucleotide antiviral agents. For example, we reported recently that 16mer OMe/LNA oligonucleotides targeted to TAR, when delivered by cationic lipids, could inhibit HIV replication in a HeLa T4 β-galactosidase cell line (56). PNA–peptides have particularly high potential because of their dual potential for antiviral and virucidal activities and the lack of need for a transfection agent. We are now in a position to improve on such activities by carrying out structure–activity relationships with further peptide–PNA conjugates, concentrating on improving their membrane penetration and endosomal release properties.

SUPPLEMENTARY DATA

Supplementary data are available at NAR Online.

ACKNOWLEDGEMENTS

We thank Martin Fabani for helpful discussions and David Owen for advice on peptide synthesis. This work is funded in part by a grant from EC Framework 5 (contract QLK3-CT-2002-01989). Funding to pay the Open Access publication charges for this article was provided by the EC Framework 5 grant.

Conflict of interest statement. None declared.

REFERENCES

1. Bennett,C.F., Chiang,M.-Y., Chan,H., Shoemaker,J.E.E. and Mirabelli,C.K. (1992) Cationic lipids enhance cellular uptake and activity of phosphorothioate antisense oligonucleotides. *Mol. Pharmacol*., **41**, 1023–1033.
2. Egholm,M., Buchardt,O., Christensen,L., Behrens,C., Freier,S.M., Driver,D.A., Berg,R.H., Kim,S.K., Norden,B. and Nielsen,P. (1993) PNA hybridizes to complementary oligonucleotides obeying the Watson–Crick hydrogen bonding rules. *Nature*, **365**, 566–568.
3. Summerton,J., Stein,D., Huang,S.B., Matthews,P., Weller,D.D. and Partridge,M. (1997) Morpholino and phosphorothioate antisense oligomers compared in cell-free and in cell systems. *Antisense Nucleic Acid Drug Dev*., **7**, 63–70.
4. Koppelhus,U., Awasthi,S.K., Zachar,V., Holst,H.U., Ebbeson,P. and Nielsen,P.E. (2002) Cell-dependent differential cellular uptake of PNA, peptides and PNA–peptide conjugates. *Antisense Nucleic Acid Drug Dev*., **12**, 51–63.
5. Lochmann,D., Jauk,E. and Zimmer,A. (2004) Drug delivery of oligonucleotides by peptides. *Eur. J. Pharm. Biopharm*., **58**, 237–251.
6. Lindsay,M.A. (2002) Peptide-mediated cell delivery: application in protein target validation. *Curr. Opin. Pharmacol*., **2**, 587–594.
7. Wadia,J.S. and Dowdy,S.F. (2002) Protein transduction technology. *Curr. Opin. Biotechnol*., **13**, 52–56.
8. Zorko,M. and Langel,U. (2005) Cell-penetrating peptides: mechanism and kinetics of cargo delivery. *Adv. Drug Deliv. Rev*., **57**, 529–545.
9. Gait,M.J. (2003) Peptide-mediated cellular delivery of antisense oligonucleotides and their analogues. *Cell. Mol. Life Sci*., **60**, 1–10.
10. Thierry,A.R., Vivès,E., Richard,J.-P., Prevot,P., Martinand-Mari,C., Robbins,I. and Lebleu,B. (2003) Cellular uptake and intracellular fate of antisense oligonucleotides. *Curr. Opin. Mol. Ther*., **5**, 133–138.
11. Zatsepin,T.S., Turner,J.J., Oretskaya,T.S. and Gait,M.J. (2005) Conjugates of oligonucleotides and analogues with cell penetrating peptides as gene silencing agents. *Curr. Pharm. Des*., **11**, 3639–3654.
12. Antopolsky,M., Azhayeva,E., Tengvall,U., Auriola,S., Jääskeläinen,I., Rönkkö,S., Honkakoski,P., Urtti,A., Lönnberg,H. and Azhayev,A. (1999) Peptide-oligonucleotide phosphorothioate conjugates with membrane translocation and nuclear localization properties. *Bioconjug. Chem*., **10**, 598–606.
13. Astriab-Fisher,A., Sergueev,D., Fisher,M., Ramsay Shaw,B. and Juliano,R.L. (2002) Conjugates of antisense oligonucleotides with the Tat and Antennapedia cell-penetrating peptides: effect on cellular uptake, binding to target sequences, and biologic actions. *Pharm. Res*., **19**, 744–754.
14. Chen,C.-P., Zhang,L.-R., Peng,Y.-F., Wang,X.-B., Wang,S.-Q. and Zhang,L.-H. (2003) A concise method for the preparation of peptide and arginine-rich peptide-conjugated antisense oligonucleotides. *Bioconjug. Chem*., **14**, 532–538.
15. Turner,J.J., Arzumanov,A.A. and Gait,M.J. (2005) Synthesis, cellular uptake and HIV-1 Tat-dependent *trans*-activation inhibition activity of oligonucleotide analogues disulphide-conjugated to cell-penetrating peptides. *Nucleic. Acids Res*., **33**, 27–42.
16. Dias,N., Dheur,S., Nielsen,P.E., Gryaznov,S., Van Aerschot,A., Herdewijn,P., Hélène,C. and Saison-Behmoaras,T.E. (1999) Antisense

PNA tridecamers targeted to the coding region of Ha-ras mRNA arrest polypeptide chain elongation. *J. Mol. Biol.*, **294**, 403–416.
17. Sazani,P., Kang,S.-H., Maier,M.A., Wei,C., Dillman,J., Summerton,J., Manoharan,M. and Kole,R. (2001) Nuclear antisense effects of neutral, anionic and cationic analogs. *Nucleic Acids Res.*, **29**, 3965–3974.
18. Karn,J. (1999) Tackling Tat. *J. Mol. Biol.*, **293**, 235–254.
19. Rana,T.M. and Jeang,K.-T. (1999) Biochemical and functional interactions between HIV-1 Tat protein and TAR RNA. *Arch. Biochem. Biophys.*, **365**, 175–185.
20. Krebs,A., Ludwig,V., Boden,O. and Göbel,M.W. (2003) Targeting the HIV *trans*-activation responsive region-approaches towards RNA-binding drugs. *Chembiochem*, **4**, 972–978.
21. Arzumanov,A., Walsh,A.P., Liu,X., Rajwanshi,V.K., Wengel,J. and Gait,M.J. (2001) Oligonucleotide analogue interference with the HIV-1 Tat protein–TAR RNA interaction. *Nucleosides Nucleotides Nucleic Acids*, **20**, 471–480.
22. Arzumanov,A., Walsh,A.P., Rajwanshi,V.K., Kumar,R., Wengel,J. and Gait,M.J. (2001) Inhibition of HIV-1 Tat-dependent *trans*-activation by steric block chimeric 2′-O-methyl/LNA oligoribonucleotides. *Biochemistry*, **40**, 14645–14654.
23. Arzumanov,A., Stetsenko,D.A., Malakhov,A.D., Reichelt,S., Sørensen,M.D., Babu,B.R., Wengel,J. and Gait,M.J. (2003) A structure-activity study of the inhibition of HIV-1 Tat-dependent *trans*-activation by mixmer 2′-*O*-methyl oligoribonucleotides containing locked nucleic acid (LNA), α-LNA or 2′-thio-LNA residues. *Oligonucleotides*, **13**, 435–453.
24. Kaushik,M.J., Basu,A. and Pandey,P.K. (2002) Inhibition of HIV-1 replication by anti-transactivation responsive polyamide nucleotide analog. *Antiviral Res.*, **56**, 13–27.
25. Pooga,M., Soomets,U., Hällbrink,M., Valkna,A., Saar,K., Rezaei,K., Kahl,U., Hao,J.-X., Xu,X.-J., Wiesenfeld-Hallin,Z. *et al.* (1998) Cell penetrating PNA constructs regulate galanin receptor levels and modify pain transmission *in vivo*. *Nat. Biotechnol.*, **16**, 857–861.
26. Kaushik,N., Basu,A., Palumbo,P., Nyers,R.L. and Pandey,V.N. (2002) Anti-TAR polyamide nucleotide analog conjugated with a membrane-permeating peptide inhibits Human Immunodeficiency Virus Type I production. *J. Virol.*, **76**, 3881–3891.
27. Chaubey,B., Tripathi,S., Ganguly,S., Harris,D., Casale,R.A. and Pandey,V.N. (2005) A PNA–Transportan conjugate targeted to the TAR region of the HIV-1 genome exhibits both antiviral and virucidal properties. *Virology*, **331**, 418–428.
28. Thomson,S.A., Josey,J.A., Cadilla,R., Gaul,M.D., Hassman,C.F., Luzzio,M.J., Pipe,A.J., Reed,K.L., Ricca,D.J., Wiethe,R.W. *et al.* (1995) Fmoc mediated synthesis of peptide nucleic acids. *Tetrahedron*, **51**, 6179–6194.
29. Holmes,S.C., Arzumanov,A. and Gait,M.J. (2003) Steric inhibition of human immunodeficiency virus type-1 Tat-dependent *trans*-activation *in vitro* and in cells by oligonucleotides containing 2′-O-methyl G-clamp ribonucleoside analogues. *Nucleic Acids Res.*, **31**, 2759–2768.
30. Vivès,E., Brodin,P. and Lebleu,B. (1997) A truncated HIV-1 Tat protein basic domain rapidly translocates through the plasma membrane and accumulates in the cell nucleus. *J. Biol. Chem.*, **272**, 16010–16017.
31. Brandén,L.J., Mohamed,A.J. and Smith,C.I. (1999) A peptide nucleic acids-nuclear localization signal fusion that mediates nuclear transport of DNA. *Nat. Biotechnol.*, **17**, 784–787.
32. Braun,K., Peschke,P., Pipkorn,R., Lampel,S., Wachsmuth,M., Waldeck,W., Friedrich,E. and Debus,J. (2002) A biological transporter for the delivery of peptide nucleic acids (PNAs) to the nuclear compartment of living cells. *J. Mol. Biol.*, **318**, 237–243.
33. Soomets,U., Kilk,T. and Langel,U. (2001) Transportan, its analogues and their applications. In Epton,R. (ed.), *Innovations and Perspectives in Solid Phase Synthesis and Combinatorial Libraries 2000*. Mayflower Press, Kingswinford, UK, pp. 131–136.
34. Siwkowski,A.M., Malik,L., Esau,C.C., Maier,M.A., Wancewicz,E.V., Albertshofer,K., Monia,B.P., Bennett,C.F. and Eldrup,A.B. (2004) Identification and functional validation of PNAs that inhibit murine CD40 expression by redirection of splicing. *Nucleic Acids Res.*, **32**, 2695–2706.
35. Allinquant,B., Hantraye,P., Mailleux,P., Moya,K., Bouillot,C. and Prochiantz,A. (1995) Downregulation of amyloid precursor protein inhibits neurite outgrowth *in vitro*. *J. Cell Biol.*, **128**, 919–927.
36. Moulton,H.M., Nelson,M.H., Hatlevig,S.A., Reddy,M.T. and Iversen,P.L. (2004) Cellular uptake of antisense morpholino oligomers conjugated to arginine-rich peptides. *Bioconjug. Chem.*, **15**, 290–299.
37. Connor,S.D. and Schmidt,S.L. (2003) Regulated portals of entry into the cell. *Nature*, **422**, 37–44.
38. De Duve,C., De Barsy,T., Poole,B., Trouet,A., Tulkens,P. and Van Hoof,F. (1974) Lysosomotropic agents. *Biochem. Pharmacol.*, **23**, 2495–2510.
39. Stewart,A.J., Pichon,C., Meunier,L., Midoux,P., Monsigny,M. and Roche,A.C. (1996) Enhanced biological activity of antisense oligonucleotides complexed with glycosylated poly-L-lysine. *Mol. Pharmacol.*, **50**, 1487–1494.
40. de Diesbach,P., N'Kuli,F., Berens,C., Sonveaux,E., Monsigny,M., Roche,A.C. and Courtoy,P.J. (2002) Receptor-mediated endocytosis of phosphodiester oligonucleotides in the HepC2 cell line: evidence for non-conventional intracellular trafficking. *Nucleic Acids Res.*, **30**, 1512–1521.
41. Ciftci,K. and Levy,R.J. (2001) Enhanced plasmid DNA transfection with lysosomotropic agents in cultured fibroblasts. *Int. J. Pharm.*, **218**, 81–92.
42. Rudolph,C., Plank,C., Lausier,J., Schillinger,U., Müller,R.H. and Rosenecker,J. (2003) Oligomers of the arginine-rich motif of the HIV-1 TAT protein are capable of transferring plasmid DNA into cells. *J. Biol. Chem.*, **278**, 11411–11418.
43. Richard,J.-P., Melikov,K., Vivès,E., Ramos,C., Verbeure,B., Gait,M.J., Chernomordik,L.V. and Lebleu,B. (2003) Cell-penetrating peptides. A re-evaluation of the mechanism of cellular uptake. *J. Biol. Chem.*, **278**, 585–590.
44. Mayhood,T., Kaushik,N., Pandey,P.K., Kashanchi,F., Deng,L. and Pandey,V.N. (2000) Inhibition of Tat-mediated transactivation of HIV-1 LTR transcription by polyamide nucleic acid targeted to the TAR hairpin element. *Biochemistry*, **39**, 11532–11539.
45. Hamma,T., Saleh,A., Huq,I., Rana,T.M. and Miller,P.S. (2003) Inhibition of HIV Tat-TAR interactions by an antisense oligo-2′-*O*-methylribonucleoside methylphosphonate. *Bioorg. Med. Chem. Lett.*, **13**, 1845–1848.
46. Folini,M., Berg,K., Millo,E., Villa,R., Prasmickaite,L., Daidone,M.G., Benatti,U. and Zaffaroni,N. (2003) Photochemical internalization of a peptide nucleic acid targeting the catalytic subunit of human telomerase. *Cancer Res.*, **63**, 3490–3494.
47. Brooks,H., Lebleu,B. and Vivès,E. (2005) Tat peptide-mediated cellular delivery: back to basics. *Adv. Drug Deliv. Rev.*, **57**, 559–577.
48. Kilk,K., Elmquist,A., Saar,K., Pooga,M., Land,T., Bartfai,T., Soomets,U. and Langel,U. (2004) Targeting of antisense PNA oligomers to human galanin receptor type 1 mRNA. *Neuropeptides*, **38**, 316–324.
49. Burlina,F., Sagan,S., Bolbach,G. and Chassaing,G. (2005) Quantification of the cellular uptake of cell-penetrating peptides by MALDI-TOF mass spectrometry. *Angew. Chem. Int. Ed. Engl.*, **44**, 4244–4247.
50. Abes,S., Williams,D., Prevot,P., Thierry,A.R., Gait,M.J. and Lebleu,B. (2005) Endosome trapping limits the efficiency of splicing correction by PNA–oligolysine conjugates. *J. Controlled Release*, in press.
51. Boulmé,F., Perälä-Heape,M., Sarih-Cottin,L. and Litvak,S. (1997) Specific inhibition of *in vitro* reverse transcription using antisense oligonucleotides targeted to the TAR regions of HIV-1 and HIV-2. *Biochim. Biophys. Acta*, **1351**, 249–255.
52. Boulmé,F., Freund,F., Moreau,S., Nielsen,P., Gryaznov,S., Toulmé,J.-J. and Litvak,S. (1998) Modified (PNA, 2′-O-methyl and phosphoramidate) anti-TAR antisense oligonucleotides as strong and specific inhibitors of *in vitro* HIV-1 reverse transcriptase. *Nucleic Acids Res.*, **26**, 5492–5500.
53. Futaki,S. (2005) Membrane-permeable arginine-rich peptides and the translocation mechanisms. *Adv. Drug Deliv. Rev.*, **57**, 547–558.
54. Tripathi,S., Chaubey,B., Ganguly,S., Harris,D., Casale,R.A. and Pandey,P.K. (2005) Anti-HIV-1 activity of anti-TAR polyamide nucleic acid conjugated with various membrane transducing peptides. *Nucleic Acids Res.*, **33**, 4345–4356.
55. Shiraishi,T., Pankratova,S. and Nielsen,P.E. (2005) Calcium ions effectively enhance the effect of antisense peptide nucleic acids conjugated to cationic Tat and oligoarginine peptides. *Chem. Biol.*, **12**, 923–929.
56. Brown,D., Arzumanov,A., Turner,J.J., Stetsenko,D.A., Lever,A.M.L. and Gait,M.J. (2005) Antiviral activity of steric-block oligonucleotides targeting the HIV-1 *trans*-activation response and packaging signal stem-loop RNAs. *Nucleosides Nucleotides Nucleic Acids*, **5-7**, 393–396.